ERDC TR-08-9

US Army Corps
of Engineers®
Engineer Research and
Development Center

Estimating Bottom Water Dissolved Oxygen in the Mississippi River Gulf Outlet and Gulf Intracoastal Waterway Resulting from Proposed Structures

Mark S. Dortch and S. Keith Martin

September 2008

Engineer Research and Development Center

ERDC/EL TR-08-9
September 2008

Estimating Bottom Water Dissolved Oxygen in the Mississippi River Gulf Outlet and Gulf Intracoastal Waterway Resulting from Proposed Structures

Mark S. Dortch

Environmental Laboratory
U.S. Army Engineer Research and Development Center
3909 Halls Ferry Road
Vicksburg, MS 39180-6199

S. Keith Martin

Coastal and Hydraulics Laboratory
U.S. Army Engineer Research and Development Center
3909 Halls Ferry Road
Vicksburg, MS 39180-6199

Final report

Prepared for U.S. Army Corps of Engineers
New Orleans District, Hurricane Protection Office
Washington, DC 20314-1000

ABSTRACT: This study examined the impacts on bottom dissolved oxygen (DO) within canal reaches comprising the Gulf Intracoastal Waterway (GIWW), the Mississippi River Gulf Outlet (MRGO), and the Inner Harbor Navigation Channel (IHNC) resulting from various alternatives for proposed water control structures located within this system. Due to time constraints, an analytical model of reduced form was used for the analysis. Bottom water DO for each canal study reach was predicted using a steady-state, fully mixed, single reactor model. August conditions were imposed for the assessment. Monthly average, bottom flushing flow rates were obtained from hourly bottom velocities output from a three-dimensional (3D) hydrodynamic and salinity model that was applied to the system during a separate study. Likewise, monthly average surface and bottom salinities were also obtained from the 3D model output. The salinity data were used to estimate vertical eddy diffusivities, which were used in the model for DO exchange between surface and bottom water. The hydrodynamic information was provided for each study reach and for each alternative scenario.

The model indicated that low DO conditions should be expected within the system for the structural alternatives being considered. The model showed that several reaches for several scenarios will have DO less than the standard of 4.0 mg/L. The IHNC reach may present a special concern since bottom DO was predicted to be 0.0 mg/L for three alternatives that included structures placed within the GIWW.

Contents

Figures and Tables

Figures

Tables

Preface

The model investigation presented in this report was authorized and funded by the U.S. Army Engineer Hurricane Protection Office (HPO), New Orleans, and was conducted by Dr. Mark Dortch of the Water Quality and Contaminant Modeling Branch (WQCMB), Environmental Processes and Effects Division (EPED), Environmental Laboratory (EL) of the U.S. Army Engineer Research and Development Center (ERDC). This report was prepared by Dr. Dortch.

This work was conducted under the general direction of Dr. Beth Fleming, Director, EL; Dr. Richard Price, Chief, EPED; and Dr. Mansour Zakikhani, acting Chief, WQCMB.

Hydrodynamic modeling that provided information to support this study was conducted by Mr. Keith Martin of the Coastal and Hydraulics Laboratory (CHL) of ERDC. Mr. Martin worked under the general direction of: Mr. Thomas W. Richardson, Director, CHL; Dr. Rose Kress, Chief of the Navigation Division, CHL; Mr. Bruce Ebersole, Chief of the Flood Protection Division, CHL; and Dr. Robert T. McAdory, Chief of the Estuarine Engineering Branch, CHL.

Dr. James R. Houston was Director of ERDC. COL Gary E. Johnston was Commander and Executive Director.

Unit Conversion Factors

Multiply	By	To Obtain
cubic feet	0.02831685	cubic meters
degrees Fahrenheit	(F-32)/1.8	degrees Celsius
feet	0.3048	meters
miles (U.S. statute)	1,609.347	meters
square feet	0.09290304	square meters

1 Introduction

Background

The Mississippi River Gulf Outlet (MRGO) Canal is a 66-mile-long deep-water navigation channel that extends northwest from the Gulf of Mexico to New Orleans, LA (Figure 1). The MRGO merges with the Gulf Intracoastal Waterway (GIWW) and continues 5 miles further to the west where it joins the Inner Harbor Navigation Canal (IHNC). The IHNC proceeds approximately 3 miles north from its intersection with the GIWW to connect with Lake Pontchartrain at Seabrook.

Various water control structures are being evaluated to reduce salinity intrusion and storm surge propagation northward. These structures cannot only affect the hydraulics and salinity of this system of channels, but they could also impact bottom dissolved oxygen (DO) due to the depths and alterations in flushing in the channels. The study presented herein was conducted to evaluate the potential impacts on DO resulting from structural alternatives being considered.

Objective

The objective of this study was to estimate summer, bottom dissolved oxygen at various locations along the MRGO, GIWW, and IHNC as a result of structural alternatives for water control being considered for this system of canals.

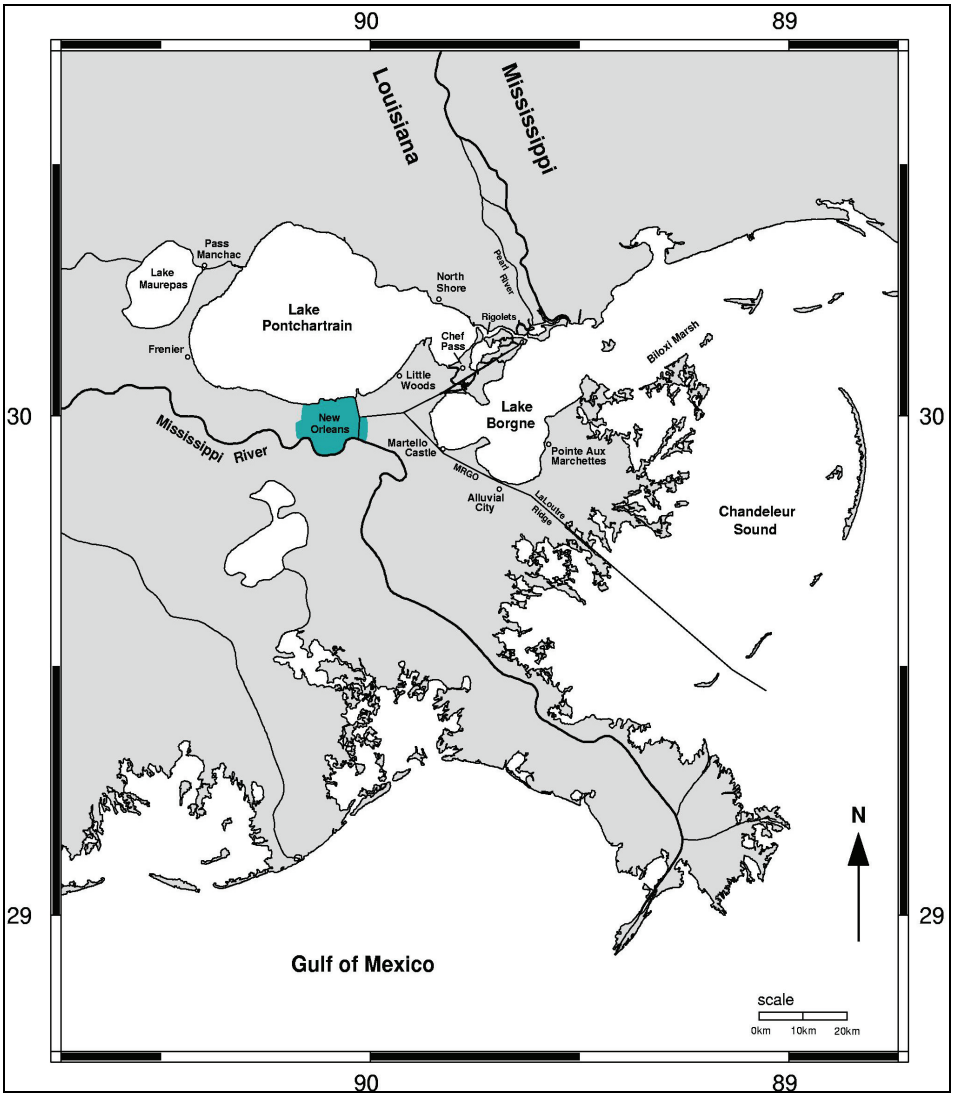

Figure 1. Vicinity map.

2 Approach

General

A screening-level analytical modeling approach was used due to the lack of availability of an adequate numerical water quality model of this system. A three-dimensional (3D) numerical hydrodynamic and water quality model of this area was developed during the Mississippi Coastal Improvement Program (MsCIP) for the U.S. Army Engineer District, Mobile (Dortch et al. 2007). However, this model did not have adequate spatial representation and resolution for the three-canal system. Due to project scheduling constraints, there was not enough time to modify the MsCIP models and re-apply them for this study. Therefore, a much simpler, screening-level approach was chosen, which consisted of an analytical mathematical model of reduced form.

The analytical approach is dependent on the flushing flow rate of aerated ambient waters from outside the canal system. The approach is bolstered by the fact that flushing flows were determined from a 3D hydrodynamic model that was being applied for the system by the Coastal and Hydraulics Laboratory (CHL), U.S. Army Engineer Research and Development Center (ERDC). Thus, there is a basis for the driving variables used in the analysis.

The analytical approach assumes steady-state, summer conditions applied to a continuously stirred tank reactor (CSTR). CSTR models are frequently used to conduct screening-level assessments of DO resulting from proposed wastewater discharges. The approach is based on the mass balance of DO and biochemical oxygen demand (BOD) at steady-state (Thomann and Mueller 1987). Concentrations are uniform in space for each constituent due to the fully mixed CSTR assumption. Thus, there is no spatial dimensionality.

The DO CSTR model is solved using a spreadsheet. For this study, the CSTR represents the bottom meter of water along the reach of the channel being assessed. A unit bottom layer thickness of 1 m was somewhat arbitrary. A bottom layer thickness was required to establish a bottom layer volume and flushing flow rate, which was based on the velocity computed

by the hydrodynamic model at the channel bottom. August conditions were applied.

Model formulation

The sources of DO are: inflow from waters entering from outside the channels, such as from the Gulf and Lake Borgne, and diffusion of aerated surface water into bottom water with lower DO. The sinks of DO are outflow due to flushing, exertion of sediment oxygen demand, and oxidation of BOD. The sources of BOD are diffusion from the surface water and in-flushing. The sinks of BOD are out-flushing and BOD loss, which is all attributed to oxidation assuming no settling of BOD. A conceptual schematic of the model formulation is shown in Figure 2.

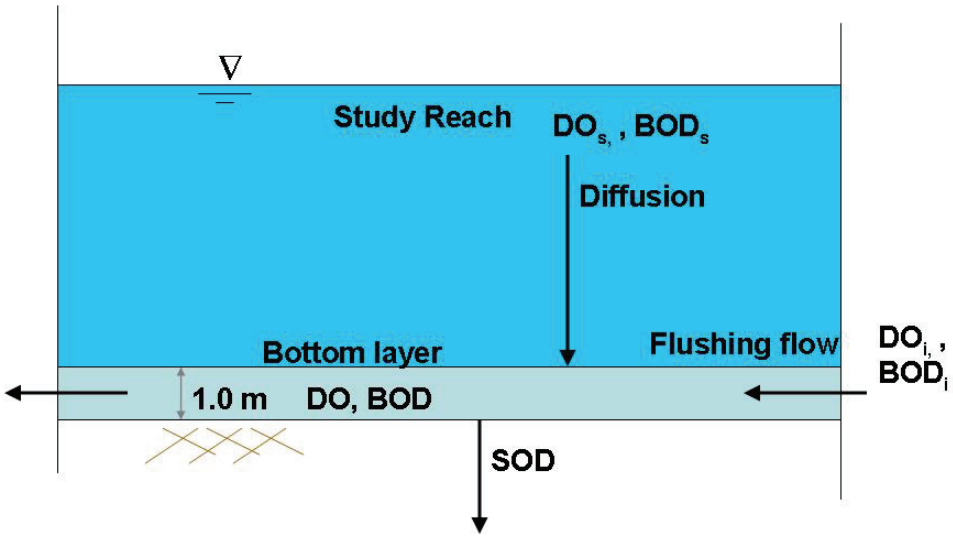

Figure 2. Model schematic.

The mass balance equations for *DO* and *BOD* are as follows:

$$V\frac{d\,DO}{d\,t} = Q\,DO_i - Q\,DO - A\;SOD + E_z^{'}\left(DO_s - DO\right) - k_1 V\,BOD \quad (1)$$

$$V\frac{d\,BOD}{d\,t} = Q\,BOD_i - Q\,BOD + E_z^{'}\left(BOD_s - BOD\right) - k_1 V\,BOD \quad (2)$$

where

DO = DO in bottom water, mg/L or g/m^3

DO_i = inflowing *DO* concentration due to flushing, mg/L or g/m^3

DO_s = *DO* concentration of surface water, mg/L or g/m^3

Q = water flushing flow rate in bottom water, m^3/day

A = surface area of the bottom water in the channel, m^2

E'_z = bulk diffusion exchange coefficient, m^3/day

SOD = sediment oxygen demand, g/m^2/day

BOD = ultimate *BOD* remaining or un-oxidized in bottom water, mg/L or g/m^3

BOD_i = inflowing ultimate *BOD* concentration due to flushing, mg/L or g/m^3

BOD_s = ultimate *BOD* concentration in surface water, mg/L or g/m^3

V = volume of the channel bottom water, m^3

t = time, days

k_1 = *BOD* decay (oxidation) rate, day^{-1}

For steady-state conditions, Equations 1 and 2 become

$$DO = DO_i - \frac{A}{Q + E'_z} SOD - \frac{k_1 V}{Q + E'_z} BOD \tag{3}$$

$$BOD = \frac{Q + E'_z}{Q + E'_z + k_1 V} BOD_i \tag{4}$$

where it is assumed that $DO_s = DO_i$ and $BOD_s = BOD_i$. Equation 4 is solved first for *BOD*, and the *BOD* solution is then used in Equation 3 to solve for *DO*.

The bulk diffusion exchange between surface and bottom water, E'_z, can be estimated as follows,

$$E'_z = \frac{E_z A}{\Delta Z} \tag{5}$$

where

A = channel surface area, m^2

ΔZ = vertical distance between the surface layer and bottom, m

E_z = vertical eddy diffusivity, m²/day

It was assumed that A is the product of the channel width at the featured cross section and the length of the channel reach under study, and ΔZ was taken as the water depth at the featured cross section. E_z in units of cm²/sec can be estimated from (Thomann and Mueller 1987)

$$E_z = 1.7x10^{-4} N^{-0.83} \tag{6}$$

where N is the stability frequency (sec^{-2}) given by

$$N = \frac{g}{\rho}\frac{\partial \rho}{\partial Z} \tag{7}$$

for g as the acceleration of gravity (9.8 m/sec²), ρ as the density of water in g/cm³, and Z as depth in m. The density of water can be computed from water temperature T (°C) and salinity S (parts per thousand, ppt) as follows (Thomann and Mueller 1987),

$$\rho = 1 + \left\{10^{-3}\left[\left(28.14 - 0.0735T - 0.00469T^2\right) + \left(0.802 - 0.002T\right)\left(S - 35\right)\right]\right\} \tag{8}$$

Equation 8 is used to compute surface and bottom water density with known temperature and salinity, and the difference in surface and bottom water density is divided by the water depth to compute N from Equation 7. The value of N is then used to compute E_z from Equation 6, and the resulting value of E_z is used to compute E'_z from Equation 5 where the resulting value is used in Equations 3 and 4. For conditions with no density difference (i.e., no salinity difference for a given temperature) between surface and bottom, E_z is infinitely large from Equation 6. So for conditions of no stratification, a value of E_z had to be specified for the model. An upper limit on E_z of 2.0 cm²/sec was set, which is consistent with values that occur with very small temperature differences between surface and bottom water that are likely to exist. A temperature difference of only a few tenths of a degree C and 20 ppt salinity can result in E_z values of about 2 cm²/sec. Similarly, a salinity difference of only 0.007 ppt results in an E_z value of 2 cm²/sec at 30 °C. Thus, an upper limit on E_z of 2.0 cm²/sec is quite reasonable.

Model implementation

The TABS-MDS 3D numerical hydrodynamic model was applied by Martin and McAlpin (2008) for the MRGO-GIWW-IHNC system. The model was re-applied for scenarios presented in this report. Information was extracted from this modeling to feed data needs for the *DO* analysis described above. Specifically, monthly average flushing rate in the bottom meter of water for each channel reach was required to set values for *Q*. August flow conditions from the 3D model at selected cross sections were used to obtain *Q*. Channel cross sections and reaches are discussed in Chapter 3. Values for *Q* were determined from the monthly time average of August hourly bottom velocities that were provided by CHL from the hydrodynamic modeling as explained in Chapter 3.

The variables *A* and *V* in Equations 3 and 4 were established as follows. A is the product of the channel width and length. The width was assumed uniform and corresponded to the width of the channel at each cross section. The channel length was equal to the entire channel reach corresponding to each cross section as discussed in Chapter 3. The bottom layer volume *V* is the product of *A* and 1.0 m. A bottom layer thickness of 1.0 m was arbitrarily set, but the goal was to prescribe a layer that is thin enough to represent the near-bottom velocity and flow. The variable ΔZ is essentially the water depth for each cross section.

The ambient dissolved oxygen of waters flushed or diffused into the bottom layer DO_i was assumed to be at a value of 80 percent of saturation for the ambient temperature and salinity. Saturation *DO* (DO_{sat}) can be computed from (Thomann and Mueller 1987)

$$DO_{sat} = Exp\left\{\begin{array}{l} -139.34411 + \dfrac{1.575701x10^{5}}{T_k} - \dfrac{6.642308x10^{7}}{T_k^{2}} + \dfrac{1.243800x10^{10}}{T_k^{3}} \\ -\dfrac{8.621949x10^{11}}{T_k^{4}} - S\left(0.017674 - \dfrac{10.754}{T_k} + \dfrac{2140.7}{T_k^{2}}\right) \end{array}\right\} \quad (9)$$

where T_k is temperature in degrees Kelvin, which is $T + 273.15$. August water temperatures for this system are typically about 30 °C based upon examination of USGS records, thus, this value was used for all scenarios. A salinity of 20.0 ppt was assumed for ambient water for all scenarios for computing DO_{sat} from Equation 9. This is the computed salinity of water in Lake Borgne for September base conditions (existing conditions without

MRGO closure) as reported by Martin and McAlpin (2008). The deviation (decrease in salinity) from this was less than 1 ppt for System A alternatives and about 2 to 3 ppt for System C alternatives. With a temperature of 30 °C and salinity of 20 ppt, 80 % DO_{sat} = 5.42 mg/L. With a decrease in salinity of 3 ppt (thus 17.0 ppt), 80 % DO_{sat} = 5.51 mg/L. Therefore, use of the higher salinity value of 20 ppt provides a conservative estimate for *DO* predictions.

Ultimate *BOD* of ambient water BOD_i must be converted from observed five-day *BOD* values BOD_5. The conversion from BOD_5 to ultimate *BOD*, BOD_u, is

$$BOD_u = \frac{BOD_5}{1 - \exp(-5k_1)} \tag{10}$$

The *BOD* decay rate is typically on the order of 0.1 day^{-1} at 20 °C, which results in a value of 2.54 for the ratio of BOD_u to BOD_5 at 20 °C. The value of k_1 used for the modeling was 0.1 day^{-1} at 20 °C ($k_{1@20}$) for all cases. Values of k_1 for other temperatures can be computed from

$$k_1 = k_{1@20}\left(1.047^{T-20}\right) \tag{11}$$

Examination of USGS records for this system indicated that BOD_5 at 20 °C varied between 1.3 and 4.0 mg/L, with a mean of about 2.5 mg/L. Thus, the input BOD_5 at 20 °C for ambient water for all scenarios was set to 2.5 mg/L. Equation 10 was used to compute BOD_u for ambient water (BOD_i) using Equation 11 to compute k_1 at 30 °C. The resulting BOD_i for all conditions was 4.57 mg/L.

Surface and bottom salinities predicted from the 3D hydrodynamic model for each scenario were used to estimate vertical eddy diffusivity (see Equations 6-8). The temperature value used in Equation 8 was assumed to be 30.0 °C for all scenarios since temperature has a relatively minor effect on water density when there are variations in salinity.

Typical values of SOD for marine waters range from about 0.5 to 2.0 $g/m^2/day$ (Chapra 1997). A value of 1.0 at 20 °C was assumed for all scenarios. SOD at 20 °C (SOD_{20}) is converted to SOD at ambient temperature according to

$$SOD = SOD_{20}\left(1.074^{T-20}\right) \quad (12)$$

The value of *SOD* at 30 °C for all conditions tested is 2.04 g/m²/day.

Reach-specific variables included:

- Channel length, width, and depth
- Bottom flushing flow rate
- Surface and bottom salinity

The channel length, width, and depth were based upon cross-section characteristics as described in the next chapter. Bottom flushing flow rate and surface and bottom salinity were obtained from the 3D hydrodynamic model and varied for each scenario. These values are also described in the next chapter.

3 Model Application

Scenario descriptions

The various scenario conditions simulated are described and summarized in Table 1. The proposed structures referenced in Table 1 are shown in Figures 3 and 4. Mesh elevations used in the hydrodynamic model and shown in Figures 3 and 4 are in units of feet. It should be noted that the base condition included the MRGO closure at la Loutre as shown in Figure 4. Also, the Seabrook structure modification is an alternative for Systems A and C, but this structure is only shown in Figure 4. Bottom water DO was computed for each of the scenarios listed in Table 3 and for each canal reach described in the next section.

Table 1. Scenario conditions.

DO Scenario	Hydrodynamic modeling scenario	Conditions
1	Base	MRGO closure at la Loutre
2	A1	Base plus MRGO closure just south of Bayou Bienvenue
3	A2	A1 plus Bienvenue sail through structure
4	A3	A2 plus sail through structure on GIWW east of Michoud Canal
5	A4	A3 plus structure on IHNC at Seabrook
6	C2	Base plus Paris Rd structure on GIWW
7	C3	C2 plus structure on IHNC at Seabrook

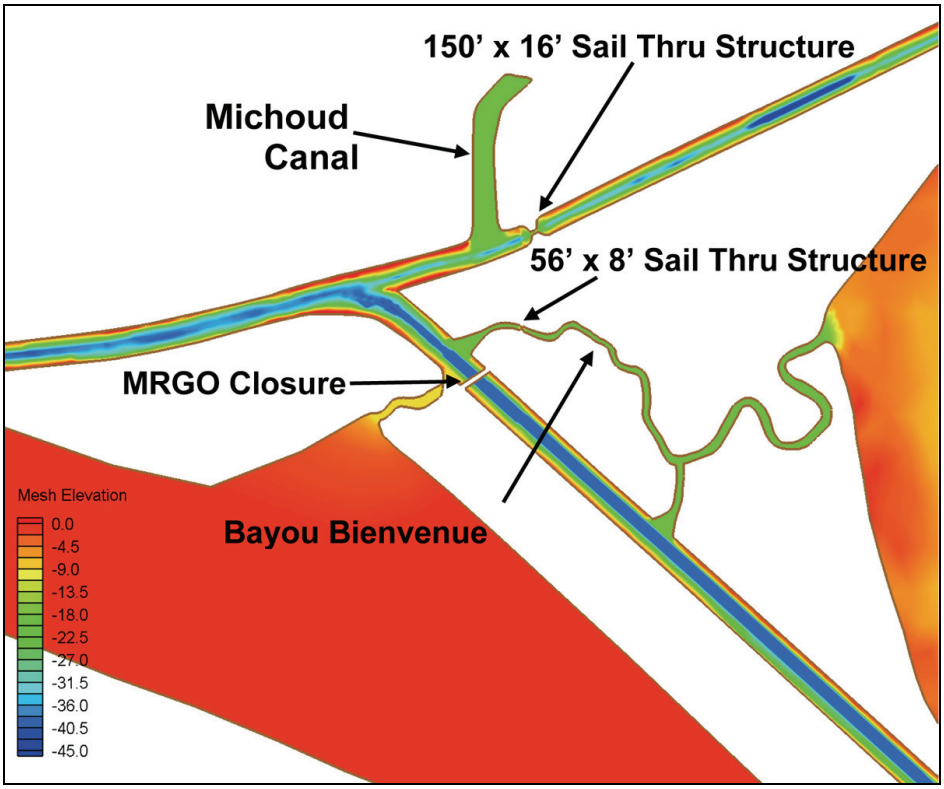

Figure 3. Proposed structures, system A.

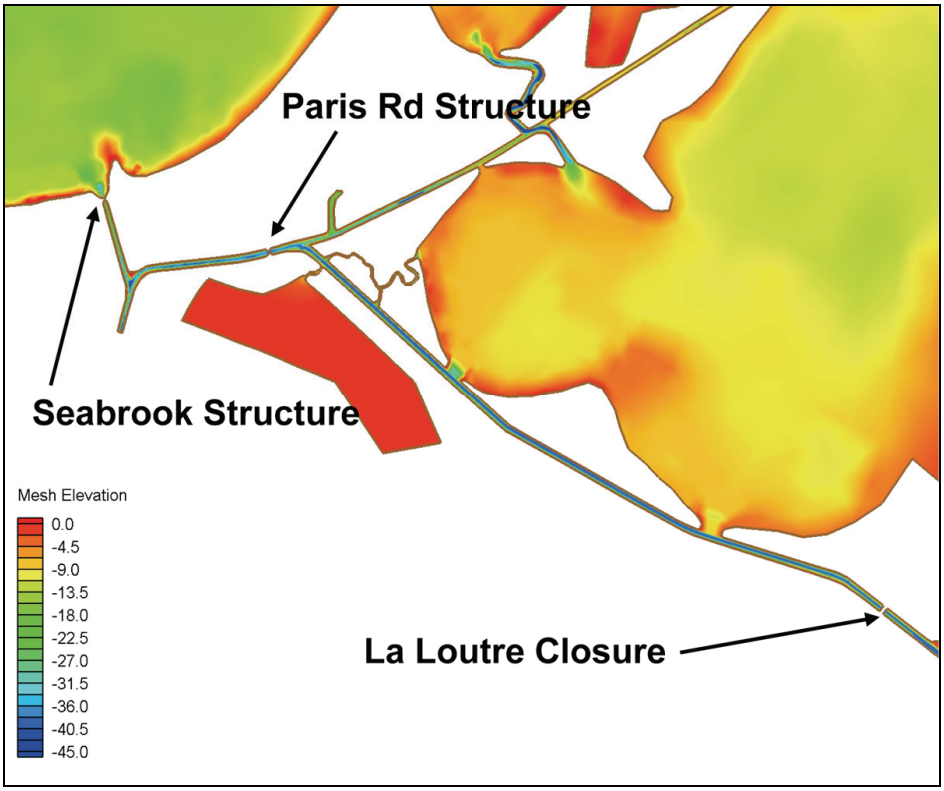

Figure 4. Proposed structures, system C.

Study reaches

Hydrodynamic output, including cross-sectional residual flows, bottom velocities, and surface and bottom salinity, were provided by CHL at select cross sections as shown in Figure 5. Bottom *DO* was computed for reaches that spanned each of these cross sections. As stated previously, it was necessary to define a study reach in order to provide the reactor length, width, and volume required to compute *DO*, which is assumed to be uniform in the reactor, or along the reach. The reach breaks were selected such that the cross sections were located between points where flow could enter or leave the canals from outside the system or where a canal ended. Thus, each reach break was located where either a structure is proposed, a canal has a bifurcation, or where there is a water passage to/from the canal from outside, such as connection to Lake Borgne or Bayou Bienvenue. Reach breaks are also shown in Figures 6 and 7.

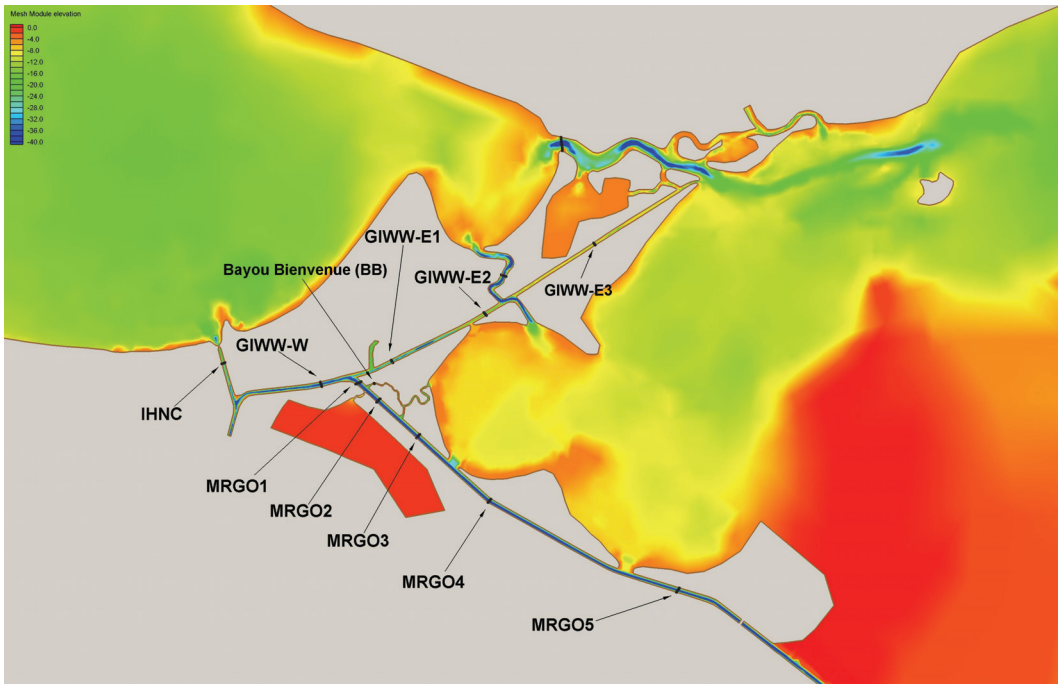

Figure 5. Cross sections for hydrodynamic output.

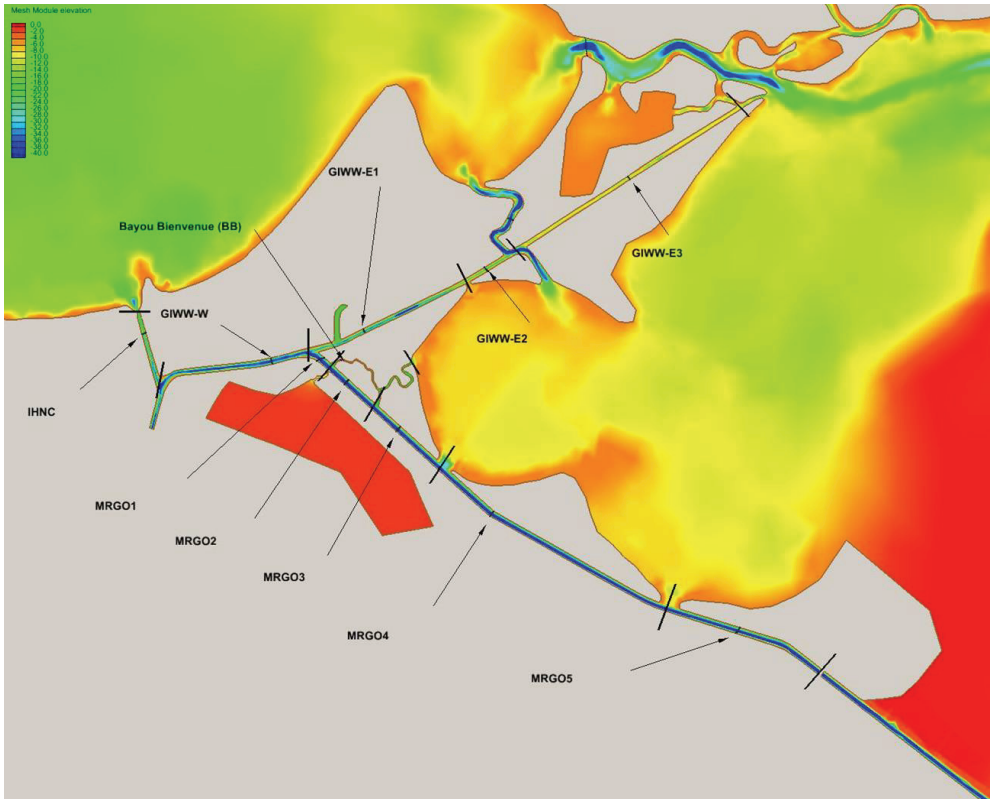

Figure 6. Reach break locations.

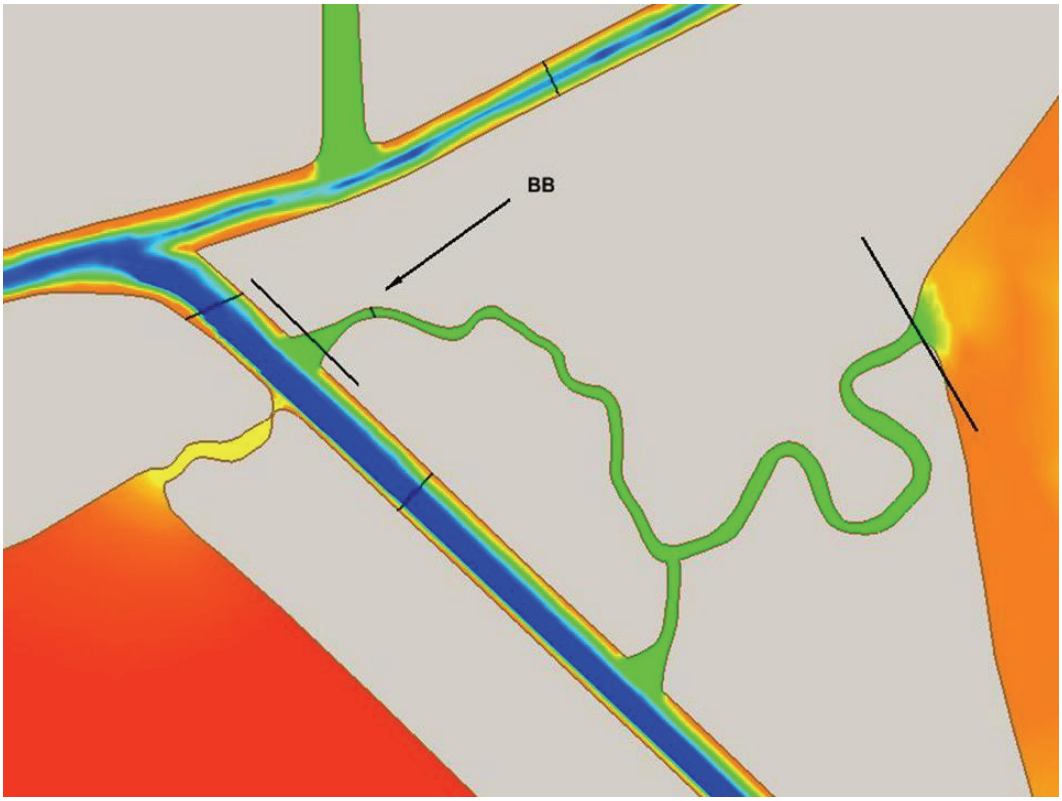

Figure 7. Reach break locations for Bayou Bienvenue.

Version 10 of the Surface Water Modeling System (Surface Modeling System (SMS) 2002) was used to estimate reach lengths. Channel widths at cross-section locations were provided by CHL from hydrodynamic model geometric inputs and correspond to widths at the channel bottom. These widths were assumed to be representative of the entire channel reach. The channel width and reach length were used to compute reach surface area. The area was multiplied times the layer depth of 1.0 m (for bottom water) to compute reach volume. The reach lengths, widths, surface areas, and bottom water volumes are shown in Table 2. With 11 study reaches and 7 scenarios, there are 77 different combinations that required 77 spreadsheets to calculate bottom water *DO* for each reach and each scenario.

Table 2. Reach geometries.

Study reach	Length, m	Width, m	Surface area, m^2	Volume, m^3
GIWW-W	9,264	260	2,411,414	2,411,414
GIWW-E1	10,691	141	1,508,162	1,508,162
GIWW-E2	3,654	113	414,577	414,577
GIWW-E3	16,355	59	960,919	960,919
MRGO-1	1,664	156	259,967	259,967
MRGO-2	3,511	150	527,508	527,508
MRGO-3	5,489	154	845,530	845,530
MRGO-4	16,423	159	2,617,115	2,617,115
MRGO-5	10,388	122	1,265,663	1,265,663
BB	8,325	75	624,251	624,251
IHNC	4,782	130	622,657	622,657

Hydrodynamic conditions

The hydrodynamics for each scenario and each cross section were provided by CHL. These consisted of hourly bottom velocities, hourly unfiltered total cross-sectional flows (bank to bank and surface to bottom), hourly filtered total cross-sectional flows, and monthly averaged surface and bottom salinities for the month of August. The bottom velocities were archived from the bottom-most node of the 7-node vertical mesh. The filtered flows had tidal components that were filtered out using a program that employed a Fast Fourier Transform method and a boxcar filter.

For each cross section and each scenario condition, monthly averages of the hourly, filtered, cross-sectional flows were nearly equivalent to the unfiltered values, as was expected. Thus, it was reasonable to simply average the bottom velocities to obtain the monthly average residual velocities.

These residual velocities were multiplied by the channel bottom width of the cross section and 1.0 m of depth to obtain the residual bottom flow needed for the *DO* analysis.

The monthly averages of the hourly, filtered cross-sectional flows are shown in Table 3 for each scenario and each cross section, where positive flow is in the northward and westward directions, i.e., towards Lake Pontchartrain. The residual flows seem reasonable for each of the cross sections and scenarios. There is a consistently small flow for the MRGO5 cross section for all scenarios, all of which included MRGO closure at la Loutre. A net zero cross-sectional residual flow is expected for this cross section since flow can only enter and leave at one location. The total residual flow is small, but not exactly zero, which can occur when computing Eulerian residual flows (Dortch et al. 1991). The flows for cross section MRGO4 are quite large and consistent for all scenarios as expected since there are two inlets from Lake Borgne to supply water for all scenarios. Also as expected, flows are greatly reduced for MRGO1 and MRGO2 for Scenarios 2 – 5, which included closure of the MRGO below Bayou Bienvenue. Adding the sail-through structure on the GIWW east of Michoud Canal (Scenarios 4 and 5) reduces flows for GIWW-E1 as one would expect. Adding the Seabrook structure (Scenarios 5 and 7) reduces flows at GIWW-W and IHNC, which also seems reasonable. Furthermore, System C (Scenarios 6 and 7) causes sizable reverse cross-sectional flows at GIWW-E1, MRGO1, MRGO2, and BB compared to System A flows.

Table 3. Total cross-sectional residual flows, m^3/sec, for August.

Cross-section Scenario	GIWW-W	GIWW-E1	GIWW-E2	GIWW-E3	MRGO1	MRGO2	MRGO3	MRGO4	MRGO5	BB	IHNC
1 (Base)	5.4	-28.1	7.6	-19.5	33.1	65.4	111.5	420.9	-1.6	-30.7	6.6
2 (A1)	6.7	5.5	30.9	-17.8	0.8	-0.3	72.7	422.0	-1.6	2.2	7.8
3 (A2)	2.5	2.9	25.0	-15.5	-1.0	-0.3	73.0	421.4	-1.7	0.3	3.0
4 (A3)	0.8	0.2	23.1	-16.1	0.2	-0.3	73.4	422.5	-1.7	1.5	1.2
5 (A4)	0.1	-0.1	22.9	-16.2	-0.3	-0.3	73.1	422.5	-1.7	0.9	0.5
6 (C2)	5.4	-22.0	11.5	-19.3	26.9	52.8	107.8	421.9	-1.6	-26.1	5.7
7 (C3)	1.0	-23.5	10.2	-19.4	24.0	51.2	106.7	423.0	-1.6	-27.3	1.3

The monthly averaged bottom flows are shown in Table 4. The bottom residual flows also seem reasonable for most cross sections and scenario conditions. For example, there is a consistently small residual bottom flow for MRGO5, but it is larger than the total cross-sectional flow shown in Table 3. This is reasonable and expected since there should be some net circulation with non-zero, but reverse, surface and bottom flows that nearly cancel, thus leading to nearly zero net total flow. The positive values of the residual bottom flows indicate that flow is moving toward the lake on the bottom, and there is most likely a reverse residual flow on the surface moving towards the Gulf. This type of circulation is typical of what one would find in a no-flow, dead-end channel with a tide on the other end (Dortch et al. 1991). The closure at la Loutre creates a dead-end channel.

The bottom residual flows for MRGO4 are consistently the same and relatively large, thus supporting similar arguments presented for the total cross-sectional flow for this reach. Some bottom residual flows are larger than the total cross-sectional residual flow, such as GIWW-W. Whenever there are reversing surface and bottom flows, it is quite possible to have a surface or bottom residual flow that nearly cancels but is greater than the total flow net flow throughout the cross section.

System C bottom residual flows tend to differ substantially from System A within the GIWW and the IHNC. The bottom residual flow for System C is decreased at GIWW-W and reversed, but increased, at IHNC compared with System A.

Table 4. Bottom residual flows, m^3/sec, for August, used to compute bottom DO.

Cross-section Scenario	GIWW-W	GIWW-E1	GIWW-E2	GIWW-E3	MRGO 1	MRGO 2	MRGO 3	MRGO 4	MRGO 5	BB	IHNC
1 (Base)	34.46	-10.76	-8.71	0.17	9.46	7.85	6.27	18.87	2.56	-2.47	5.49
2 (A1)	34.56	-0.13	0.02	0.22	7.77	3.31	5.61	18.92	2.56	0.50	4.18
3 (A2)	34.57	0.01	0.20	0.25	2.64	3.27	5.43	18.90	2.78	0.01	1.26
4 (A3)	34.66	0.43	0.13	0.22	2.99	3.27	5.43	18.94	2.79	0.23	1.37
5 (A4)	34.66	0.24	0.06	0.19	2.96	3.27	5.42	18.94	2.79	0.13	1.39
6 (C2)	3.40	-0.04	-2.12	-0.56	2.78	3.75	8.04	19.18	2.53	-4.00	-8.27
7 (C3)	3.01	0.05	-2.03	-0.56	2.75	3.78	8.22	19.22	6.69	-4.35	-8.61

The flows in Table 4 were entered into each of the 77 spreadsheets to provide the flushing flow rate to compute *DO*. All data required to compute bottom *DO* have been described with the exception of water depth and surface and bottom salinities. Water depth for each cross section was determined by examining model bathymetry depths with SMS. The cross-section depths were assumed to represent the average reach depth. The depth of each reach used for *DO* modeling is shown in Table 5.

Table 5. Reach water depths.

Reach	Total depth, m
GIWW-W	11.89
GIWW-E1	10.30
GIWW-E2	6.31
GIWW-E3	4.08
MRGO1	12.19
MRGO2	12.19
MRGO3	12.19
MRGO4	12.19
MRGO5	12.19
BB	6.10
IHNC	9.14

Hourly surface and bottom salinities output by the hydrodynamic model were averaged over August for use in the DO model to compute vertical eddy diffusivities. The monthly averaged surface and bottom salinities are shown in Tables 6 and 7 for each scenario and cross section. These data complete the data input requirements for the *DO* model.

Table 6. August monthly averaged surface salinities, ppt.

Cross-section Scenario	GIWW-W	GIWW-E1	GIWW-E2	GIWW-E3	MRGO1	MRGO2	MRGO3	MRGO4	MRGO5	BB	IHNC
1 (Base)	10.789	11.654	11.811	13.302	11.752	12.435	13.315	13.658	13.028	12.083	7.296
2 (A1)	10.090	11.383	11.848	13.437	11.031	12.901	13.268	13.661	13.030	11.841	6.958
3 (A2)	11.036	12.182	12.514	13.996	12.023	13.923	14.154	14.418	13.915	12.704	8.810
4 (A3)	10.987	12.178	12.526	13.942	11.980	13.918	14.153	14.418	13.913	12.726	7.647
5 (A4)	10.685	11.929	12.380	13.826	11.681	13.706	13.951	14.230	13.686	12.456	7.543
6 (C2)	11.420	11.741	11.759	13.274	11.793	11.976	13.008	13.587	12.961	11.936	7.995
7 (C3)	11.411	11.733	11.777	13.292	11.774	11.956	13.020	13.591	12.966	11.919	8.096

Table 7. August monthly averaged bottom salinities, ppt.

Cross-section Scenario	GIWW-W	GIWW-E1	GIWW-E2	GIWW-E3	MRGO1	MRGO2	MRGO3	MRGO4	MRGO5	BB	IHNC
1 (Base)	11.544	11.656	11.800	13.310	12.354	12.750	13.316	13.658	13.026	12.244	8.269
2 (A1)	10.679	11.440	11.837	13.445	11.352	12.902	13.270	13.661	13.028	11.886	7.633
3 (A2)	11.648	12.196	12.500	14.003	12.198	13.924	14.155	14.418	13.913	12.704	10.400
4 (A3)	11.656	12.203	12.511	13.949	12.247	13.919	14.154	14.418	13.912	12.726	8.710
5 (A4)	11.357	11.964	12.366	13.834	11.963	13.706	13.953	14.230	13.684	12.456	8.459
6 (C2)	11.442	11.742	11.749	13.283	11.799	11.982	13.082	13.587	12.960	11.936	9.418
7 (C3)	11.418	11.734	11.767	13.301	11.780	11.963	13.095	13.591	12.965	11.919	9.529

4 Model Results

Some general results can be drawn regarding the flows of Table 4. These observations are noteworthy since the DO responses are expected to exhibit similar patterns. For cross section GIWW-W, the only condition that seems to alter the flow from the base condition is the inclusion of the Paris Rd structure, Scenarios 6 and 7. Only minor deviations in flow for all non-base conditions are observed for cross section GIWW-E3. Cross sections MRGO1 and MRGO2 tend to exhibit about the same flows for all of the conditions, with the exception of the base condition for both and Scenario 2 for MRGO1. Cross sections MRGO3, MRGO4, and MRGO5 experience about the same flows for all conditions.

Examination of Tables 6 and 7 reveals that salinities at some of the stations are inverted, i.e., surface salinity is greater than bottom, which is the case for all scenarios at cross section MRGO5, where a very slight inversion can be seen. For the inverted salinity cases, it was assumed that the surface and bottom salinity was the same, which resulted in the maximum value of E_z of 2.0 cm^2/sec.

Table 8 shows the level of salinity stratification with levels of relatively high (H), low (L), and medium (M). Stratification is important since it has a strong influence on the mixing of surface water with higher *DO* into bottom water with lower *DO*. Weaker stratification is usually indicative of higher bottom *DO*, and stronger stratification is usually the reverse. Cross sections GIWW-E1, GIWW-E2, GIWW-E3, MRGO4, and MRGO5 consistently had low salinity stratification for all scenarios (except for GIWW-E1 Scenario 2). Cross section MRGO2 had low salinity stratification for all scenarios except Scenario 1. Cross Section MRGO3 had low salinity stratification for all scenarios except Scenarios 6 and 7, which exhibited medium stratification. Cross section BB had low salinity stratification for all scenarios except Scenarios 1 and 2. Cross section IHNC consistently had higher levels of salinity stratification for all scenarios. Cross sections GIWW-W and MRGO1 had relatively high salinity stratification for all scenarios except Scenarios 6 and 7.

Table 8. Levels of salinity stratification.

Reach Scenario	GIWW-W	GIWW-E1	GIWW-E2	GIWW-E3	MRGO1	MRGO2	MRGO3	MRGO4	MRGO5	BB	IHNC
1 (Base)	H	L	L	L	H	H	L	L	L	H	H
2 (A1)	H	M	L	L	M	L	L	L	L	M	H
3 (A2)	H	L	L	L	H	L	L	L	L	L	H
4 (A3)	H	L	L	L	H	L	L	L	L	L	H
5 (A4)	H	L	L	L	H	L	L	L	L	L	H
6 (C2)	L	L	L	L	L	L	M	L	L	L	H
7 (C3)	L	L	L	L	L	L	M	L	L	L	H

H = high, L = low, M = medium

Bottom *DO* values computed with the spreadsheet model are shown for each reach and each scenario in Table 9. Louisiana *DO* standards are 5.0 mg/L for freshwater and coastal marine waters with salinity less than 10 ppt and 4.0 mg/L for estuarine waters with salinity greater than 10 ppt. Since the waters in the MRGO/GIWW/IHNC are above 10 ppt for most cases except cross-section IHNC, a *DO* standard of 4.0 mg/L appears to be appropriate for comparison with results.

Table 9. Computed August bottom DO, mg/L.

Reach Scenario	GIWW-W	GIWW-E1	GIWW-E2	GIWW-E3	MRGO1	MRGO2	MRGO3	MRGO4	MRGO5	BB	IHNC
1 (Base)	3.36	4.23	4.82	4.70	4.57	3.54	4.10	4.09	3.72	1.29	2.21
2 (A1)	3.39	1.33	4.42	4.70	4.42	4.04	4.06	4.09	3.72	2.51	1.46
3 (A2)	3.39	3.81	4.44	4.77	3.03	4.03	4.04	4.09	3.74	4.46	0.00
4 (A3)	3.39	3.32	4.43	4.77	3.12	4.03	4.04	4.09	3.74	4.47	0.00
5 (A4)	3.39	2.66	4.43	4.70	3.09	4.03	4.04	4.09	3.74	4.46	0.00
6 (C2)	3.60	3.81	4.56	4.63	4.26	4.08	3.38	4.10	3.72	4.61	3.17
7 (C3)	3.69	3.81	4.55	4.63	4.25	4.09	3.40	4.10	3.97	4.62	3.26

The results indicate that only reaches GIWW-E2, GIWW-E3, and MRGO4 will have *DO* values above the standard for all scenarios. *DO* values for reaches MRGO4 and MRGO 5 are very consistent across scenarios, but MRGO5 is always slightly below the standard while MRGO4 is always slightly above. However, bottom *DO* for MRGO5 is not as low as was

expected for a dead-end channel. The lowest *DO* values were computed for reach IHNC, where *DO* of 0.0 mg/L was predicted for Scenarios 3, 4, and 5. All of the proposed structures improve *DO* along reaches GIWW-W, BB, and MRGO 2 compared to the base condition of the closure at la Loutre. *DO* for reach MRGO3 is above the standard for all scenarios except Scenarios 6 and 7. Reach GIWW-W consistently exhibits *DO* less than the standard for all scenarios. The IHNC reach exhibits the lowest computed bottom *DO* that is below the standard for all scenarios as well.

The bottom *DO* values for each reach were averaged across all scenarios and are reported in Table 10 in the rank order of lowest to highest. Reach GIWW-E3 exhibited the highest average bottom *DO* for all scenarios with an average value of 4.70 mg/L, while reach IHNC exhibited the lowest with an average of 2.03 mg/L.

Table 10. Reach bottom DO averaged across all scenarios.

Reach	Average DO, mg/L
IHNC	2.03
GIWW-E1	3.28
GIWW-W	3.46
MRGO5	3.76
BB	3.77
MRGO1	3.82
MRGO3	3.87
MRGO2	3.98
MRGO4	4.09
GIWW-E2	4.52
GIWW-E3	4.70

The bottom *DO* values for each scenario were averaged across all reaches and are reported in Table 11 in the rank order of lowest to highest. Scenario 7, with a value of 4.03 mg/L, was the only one with an average *DO* greater than 4.0 mg/L. Scenario 2 had the lowest *DO* average across all reaches. However, the range in average bottom *DO* shown in Table 11 for all the scenarios is rather small, indicating that there is not a noteworthy difference in system averages among the scenarios.

Sensitivity testing revealed that for weak salinity stratification the surface and bottom salinity values had a much greater impact on bottom *DO*, due to the amount of vertical diffusion, than did variations in bottom flushing flow rate. Considering reach MRGO5 and Scenario 1 for example, a tenfold decrease in vertical eddy diffusivity decreased bottom *DO* from 3.72 to 0.0 mg/L,

Table 11. Scenario bottom DO averaged across all reaches.

Scenario	Average DO, mg/L
2	3.47
5	3.51
4	3.58
1	3.69
3	3.99
6	3.99
7	4.03

whereas a tenfold decrease in the bottom flushing flow rate only decreased bottom *DO* to 3.54 mg/L. Similar results were found for other reaches and scenarios. However, for relatively strong salinity stratification, the reverse is true, i.e., bottom flushing flow rate has more effect on bottom *DO* than does vertical stratification. For example, considering Scenario 1 and reach IHNC, a tenfold decrease in vertical eddy diffusivity only decreased bottom *DO* from 2.21 to 1.98 mg/L, whereas a tenfold decrease in the bottom flushing flow rate decreased bottom *DO* to 0.0 mg/L. Thus, the bottom *DO* is more sensitive to vertical stratification and vertical mixing than canal flushing rate for weak stratification, but it is more sensitive to flushing flow rate than stratification under more stratified conditions. However, it should be recognized that the level of salinity stratification and the flushing flows are interrelated; flow affects stratification and vice versa.

A review of observed *DO* furnished by the HPO revealed that there have been times when the *DO* was relatively low. For example, *DO* observed on September 21, 2005 was 3.0 mg/L in the IHNC. Also, *DO* was observed to vary between 4 and 5 mg/L during the summer and early fall of 1974 with a value as low as 3.6 mg/L on July 8, 1974 at a GIWW station near Paris Rd. The depth at which these measurements were taken was not reported. It appears that the canal system has some history of low *DO* even with the MRGO fully open, which is expected to provide greater circulation and flushing and thus higher *DO* than conditions examined under the study scenarios.

All of the scenarios were run with a bottom in-flushing *DO* boundary condition of 80 percent *DO* saturation, which assumes that relatively well aerated water enters the reach from outside the canal system. However, there are several reaches in the system, such as GIWW-W, MRGO1, and MRGO2 that are not connected with outside water, rather they are sandwiched between other canal reaches. For such reaches, the in-flushing *DO* can come from the adjacent reach rather than outside the canal system, and the in-flushing *DO* may be less than 80 percent of saturation. Thus, the actual bottom *DO* for inner reaches may be less than estimated here. Most of the study reaches have end-points that are located at a junction with an outside water body where in-flushing *DO* is expected to be higher.

5 Conclusions and Recommendations

The analytical model for canal bottom *DO* indicated that low *DO* conditions should be expected within the bottom waters of the system for the structural alternatives being considered. The model showed that several reaches for several scenarios will have bottom *DO* less than the standard of 4.0 mg/L. The IHNC reach may present a special concern since bottom *DO* was predicted to be 0.0 mg/L for three alternatives.

Scenario 7 appears to provide the best overall *DO* of the seven alternatives that were evaluated, while Scenario 2 provided the worst. However, the range in system average bottom *DO* was quite small among the scenarios. Additionally, with the exception of the IHNC reach, the variation in *DO* among the various reaches and scenarios was not very great, especially when contrasted against the *DO* model uncertainty. Thus, decisions regarding which structures to build should probably not rest on the results of this *DO* analysis alone.

There were a number of assumptions in the development and implementation of the *DO* model as discussed in Chapters 2 and 3 that affect the model uncertainty. For example, it was assumed that the *DO* of ambient water that mixes down from the surface and flushes into the canals from external waters was at 80-percent saturation for an ambient temperature and salinity of 30 ^{o}C and 20 ppt, respectively, yielding an ambient *DO* value of 5.42 mg/L. An assumed saturation of 80 percent is reasonable, but actual values could be higher or lower.

It was assumed that in-flushing *DO* came from outside the system at 80-percent saturation, whereas for some inner reaches, the inflowing water and *DO* can come from an adjacent reach that can have lower *DO*. In these cases, the actual bottom *DO* could be less than the estimates presented. A potential refinement to the model would be to consider flushing from adjacent reaches rather than from outside waters for the inner, isolated reaches.

Salinity of ambient water may be several parts per thousand lower with proposed structures in place, which will result in slightly higher ambient

DO (approximately 0.1 mg/L higher); but such a refinement changes *DO* results less than measurement error.

Sediment oxygen demand could be higher or lower than the assumed value of 1.0 g/m^2/day at 20 ^{o}C, but a value of 1.0 is quite reasonable. The upper limit of vertical eddy diffusivity was set at 2.0 cm^2/sec, which is reasonable based upon the existence of the slightest temperature difference between surface and bottom water.

Results are more sensitive to salinity stratification for weak stratification and more sensitive to canal flushing flow rate for stronger stratification. However, it should be recognized that stratification and flushing flow are co-dependent.

Salinity stratification and canal bottom water flushing flow rates were the only scenario-dependent input variables, and both were extracted from the 3D hydrodynamic model. Use of these inputs helped to reduce model uncertainty. Potential improvements could be made to the model, such as considering bottom *DO* from adjacent reaches for in-flushing *DO* for inner, isolated reaches. However, the best approach for minimizing model error and uncertainty would be to apply a fully 3D water quality model, coupled to a 3D hydrodynamic model. Application of a 3D water quality model would greatly reduce the number of assumptions and uncertainty while providing time-varying responses with much greater spatial resolution. However, it is advisable to have access to quality observational data sets for model calibration and validation when applying comprehensive numerical water quality models, and it appears that this system may be lacking adequate observational data at this time for such applications. It would be prudent to begin collection of sufficient field water quality data to support more detailed future model-based analyses with less uncertainty.

The screening-level model described herein provides first-order estimates of bottom *DO* impacts resulting from various structural alternatives within the canals. Given the model simplicity, these *DO* results should not be used as exact predictions, rather the results are indicative of what to expect. In this case, the modified canal system is expected to experience bottom *DO* that is less than state standards at multiple locations during the summer.

References

Chapra, S. C. 1997. *Surface water quality modeling*. New York, NY: McGraw-Hill.

Dortch, M. S., R. S. Chapman, and S. R. Abt. 1991. Application of three-dimensional, Lagrangian residual transport. *J. Hydraulic Engineering*, ASCE 118(6): 831-848.

Dortch, M.S., M. Zakikhani, M. R. Noel, and S. C. Kim. 2007. *Application of a water quality model to Mississippi Sound to evaluate impacts of freshwater diversions*. ERDC/EL TR-07-20. Vicksburg, MS: U.S. Army Engineer Research and Development Center.

Martin, S. K., and T. O. McAlpin. 2008. *Flood gate analysis of the Mississippi River Gulf Outlet and Gulf Intracoastal Waterway*. Draft technical report. Vicksburg, MS: U.S. Army Engineer Research and Development Center.

Surface Modeling System (SMS). 2002. Version 8.0 Reference Manual for the Surface Water Modeling System. Provo, Utah: Brigham Young University, Engineering Graphics Laboratory. http://www.ems-i.com/

Thomann, R. V., and J. A. Mueller. 1987. *Principles of surface water quality modeling and control*. New York, NY: HarperCollins Publishers.

REPORT DOCUMENTATION PAGE

Form Approved
OMB No. 0704-0188

1. REPORT DATE *(DD-MM-YYYY)*	**2. REPORT TYPE**	**3. DATES COVERED** *(From - To)*
September 2008	Final report	

4. TITLE AND SUBTITLE
Estimating Bottom Water Dissolved Oxygen in the Mississippi River Gulf Outlet and Gulf Intracoastal Waterway Resulting from Proposed Structures

5a. CONTRACT NUMBER

5b. GRANT NUMBER

5c. PROGRAM ELEMENT NUMBER

6. AUTHOR(S)

Mark S. Dortch and S. Keith Martin

5d. PROJECT NUMBER

5e. TASK NUMBER

5f. WORK UNIT NUMBER

7. PERFORMING ORGANIZATION NAME(S) AND ADDRESS(ES)

U.S. Army Engineer Research and Development Center
Environmental Laboratory and Coastal and Hydraulics Laboratory
3909 Halls Ferry Road
Vicksburg, MS 39180-6199

8. PERFORMING ORGANIZATION REPORT NUMBER

ERDC TR-08-9

9. SPONSORING / MONITORING AGENCY NAME(S) AND ADDRESS(ES)

Headquarters, U.S. Army Corps of Engineers
Washington, DC 20314-1000

10. SPONSOR/MONITOR'S ACRONYM(S)

11. SPONSOR/MONITOR'S REPORT NUMBER(S)

12. DISTRIBUTION / AVAILABILITY STATEMENT
Approved for public release; distribution is unlimited.

13. SUPPLEMENTARY NOTES

14. ABSTRACT

This study examined the impacts on bottom dissolved oxygen (DO) within canal reaches comprising the Gulf Intracoastal Waterway (GIWW), the Mississippi River Gulf Outlet (MRGO), and the Inner Harbor Navigation Channel (IHNC) resulting from various alternatives for proposed water control structures located within this system. Due to time constraints, an analytical model of reduced form was used for the analysis. Bottom water DO for each canal study reach was predicted using a steady-state, fully mixed, single reactor model. August conditions were imposed for the assessment. Monthly average, bottom flushing flow rates were obtained from hourly bottom velocities output from a three-dimensional (3D) hydrodynamic and salinity model that was applied to the system during a separate study. Likewise, monthly average surface and bottom salinities were also obtained from the 3D model output. The salinity data were used to estimate vertical eddy diffusivities, which were used in the model for DO exchange between surface and bottom water. The hydrodynamic information was provided for each study reach and for each alternative scenario.

The model indicated that low DO conditions should be expected within the system for the structural alternatives being considered. The model showed that several reaches for several scenarios will have DO less than the standard of 4.0 mg/L. The IHNC reach may present a special concern since bottom DO was predicted to be 0.0 mg/L for three alternatives that included structures placed within the GIWW.

15. SUBJECT TERMS

Dissolved oxygen
Gulf Intracoastal Waterway
Inner Harbor Navigation Channel
Mississippi River Gulf Outlet
Model

16. SECURITY CLASSIFICATION OF:			**17. LIMITATION OF ABSTRACT**	**18. NUMBER OF PAGES**	**19a. NAME OF RESPONSIBLE PERSON**
a. REPORT	**b. ABSTRACT**	**c. THIS PAGE**			**19b. TELEPHONE NUMBER** *(include area code)*
UNCLASSIFIED	UNCLASSIFIED	UNCLASSIFIED		32	